

High Temperature Fracture Toughness and Fatigue Behavior of

Ti-Zr-Mo and W-Re Alloys for X-ray Tube Application

(X線管に用いる Ti-Zr-Mo および W-Re 合金の高温破壊じん性と疲労挙動)

MOHD AZHAR BIN HARIMON

14700581

Supervisor: Associate Professor Yukio Miyashita

A dissertation submitted in partial fulfillment of the requirements for the degree of

Doctor of Engineering in Materials Science

Department of Materials Science and Engineering

Nagaoka University of Technology

Nagaoka, Niigata, Japan

December, 2017

High Temperature Fracture Toughness and Fatigue Behavior of Ti-Zr-Mo and W-Re Alloys for X-ray Tube Application

(X線管に用いる Ti-Zr-Mo および W-Re 合金の高温破壊じん性と疲労挙動)

Approved by:

Dr. Yoshiharu Mutoh
Professor Emeritus
Nagaoka University of Technology

Dr. Yukio Miyashita
Department of Mechanical Engineering
Nagaoka University of Technology

Dr. Yuichi Otsuka
Department of System Safety
Nagaoka University of Technology

Dr. Masakazu Okazaki
Department of Mechanical Engineering
Nagaoka University of Technology

Dr. Yutaka Hiraoka
Specially-appointed Professor
Okayama University of Science

ACKNOWLEDGEMENTS

First of all, I would like to thank for my advisor, Associate Prof. Yukio Miyashita for kindly support, advice and all of the contributions for me during my studying and doing the research work in the doctoral program.

My pleasure to thank Prof. Emeritus Yoshiharu Mutoh, who gave me the opportunity and a contribution for studying in a doctoral program in Nagaoka University of Technology (NUT), and valuable comments and suggestions on my research work.

I would like to thank Associate Prof. Yuichi Otsuka for kindly support, comments and discussions on my research work and presentations at seminars in every week.

I also wish to express my sincere thank to the doctoral examination committee members Prof. M. Okazaki, and Prof. Y. Hiraoka for their time, valuable comments and useful suggestions on my thesis work. I also wish to express my gratitude to Toshiba Materials Co. Ltd. and Mr. S. Yamamoto for providing me sufficient specimens to conduct my experimental work.

I would like to thank Mr. Hoshino and all of machine shop staffs for everything that they kindly supported for my experimental works. For all of the lab members, I would like to thank for giving me a warm welcome, kindness, and good memories while I was spending my life in Japan. I will remember all of you.

Particularly, I am grateful for the Universiti Tun Hussein Onn Malaysia and Malaysian Government Scholarship for financial support during the period of the doctoral program.

Finally, I would like to especially thank my lovely wife Norhuda, children, family and friends for their love, support, and encouragement.

MOHD AZHAR BIN HARIMON

ABSTRACT

Commercial x-ray targets for computed tomography (CT) applications consist of two major components, a metal disc made of the titanium-zirconium-molybdenum (TZM) alloy, and a surface layer in the bombarding region made of the tungsten-rhenium (W-Re) alloy. The target must endure extremely high temperature, associated with high thermal stress, and mechanical stress due to the centrifugal force induced by high speed rotation of the target. Therefore, studies on high temperature fracture and fatigue behavior of these materials would be the most important for reliability assessment and safety design of the x-ray target. However, they have been rarely reported and high temperature fracture and fatigue behavior of these materials has been not always clarified.

In the present study, high temperature fracture toughness was evaluated for two kind of TZM alloys, one with higher C content and the other with higher O content. Moreover, effect of forging rate on high temperature fracture toughness was discussed. Fatigue properties at room temperature and 1000 °C were evaluated for three kinds of materials, layered W-Re/TZM, bulk W-Re and bulk TZM, and a fatigue failure definition in the high temperature fatigue test was investigated to evaluate high temperature fatigue strength. The fatigue processes of these x-ray target materials at high temperature were also investigated.

High temperature fracture toughness of two TZM alloys with different kinds of grain boundary particles was successfully evaluated using the convenient J_{IC} test method. The result indicated that the J_{IC} values at temperatures ranged from 800 °C to 1000 °C were almost constant regardless of temperature, while the J_{IC} values of the TZM with

higher C content were higher than those of the TZM with higher O content. The TZM with different forging rates showed similar J_{IC} values, which suggested the effect of forging rate would be not significant at high temperatures.

High temperature fatigue characteristics of W-Re and TZM were successfully evaluated under load-controlled four point bending test at 1000 °C by introducing a fatigue failure criterion as two-times increase of initial compliance, which was corresponding to nucleation and propagation of multiple cracks from specimen surface. The layered W-Re/TZM specimen exhibited the similar fatigue strength to the bulk W-Re specimen. The bulk TZM showed much lower fatigue strength compared to the layered W-Re/TZM and the bulk W-Re. The total crack length measured on the specimen surface at 1000 °C would be a dominant indicator for evaluating progress of fatigue damage.

Table of Contents

Acknowledgement	i
Abstract	ii
Table of Contents	iv
List of Figures	viii
List of Tables	xiii
List of Publications and Conferemces	xiv
Chapter 1 Introduction	
1.1 Introduction to refractory metals	1
1.1.1 Molybdenum	3
1.1.1.1 TZM alloy	3
1.1.2 Tungsten	4
1.1.2.1 Tungsten-rhenium alloy	5
1.1.3 Fabricating process of refractory metals	6
1.2 Application of refractory metals	8
1.2.1 X-ray tube application	10

1.2.2	Critical issues in x-ray tube design	16
1.2.3	Speculated fracture process of x-ray tube	17
1.3	Current status of research on high temperature fracture toughness and fatigue behavior of tungsten/molybdenum alloys	19
1.3.1	Fracture toughness at high temperature	19
1.3.2	Fatigue properties at high temperature	23
1.4	Objective of the present study	26
1.5	Dissertation outline	27
	References	29
Chapter 2	High temperature fracture toughness of TZM alloys	
2.1	Introduction	38
2.2	Experimental procedure	40
2.2.1	Materials	40
2.2.2	Fracture toughness test	43
2.3	Results and discussion	46
2.3.1	Determination of side-groove depth	46

2.3.2	High temperature fracture toughness	48
2.3.3	Effect of forging rate on fracture toughness	51
2.3.4	Fracture surface observation	52
2.3.5	Fracture toughness consideration in x-ray tube design	54
2.4	Conclusions	56
	References	57
Chapter 3	High temperature fatigue characteristics of W-Re and TZM Alloys	
3.1	Introduction	60
3.2	Experimental procedure	65
3.2.1	Materials	65
3.2.2	Fatigue test	68
3.2.2.1	Fatigue specimen	68
3.2.2.2	Fatigue test at room temperature	70
3.2.2.3	Fatigue test at 1000 °C	71
3.3	Results and Discussion	77
3.3.1	Fatigue behavior at room temperature	77
3.3.2	Fatigue behavior at 1000 °C	79

	3.3.2.1 S-N curve at 1000 °C	79
	3.3.2.2 Fatigue fracture process observations at 1000 °C	80
	3.3.2.3 Fatigue crack propagation mechanism	88
	3.3.3 Remaining fatigue life at room temperature after high temperature fatigue test	90
3.4	Conclusions	94
	References	96
Chapter 4	Conclusions	
4.1	Background	103
4.2	Barriers to be solved for achieving the present research	104
4.3	Characteristics of high temperature fracture toughness of TZM	104
4.4	Characteristics of fatigue behavior of W-Re and TZM	105
4.5	Future works	106

List of Figures

Chapter 1

- Fig. 1.1 (a) Relationship of DBTT and average recrystallized grain diameter for pure tungsten and W-24Re/W-26Re and (b) relationship of Vickers hardness (VHN) and rhenium content [11]. 6
- Fig. 1.2 Fabrication processes of Mo and W components. 8
- Fig. 1.3 Recommended operating temperature range for structural materials in space nuclear power systems [3]. 9
- Fig. 1.4 Growth in advance imaging utilization rates from 1995 to 2005 [33]. 11
- Fig. 1.5 Stationary anode x-ray tube [35]. 12
- Fig. 1.6 An x-ray tube with a rotating anode target and a heated filament [36]. 13
- Fig. 1.7 Rotating anode disk [43]. 14
- Fig. 1.8 (a) Temperature distributions at the end of the exposure, and (b) the evolution of temperature at the focal track for different sizes of target and power rates, simulated by FEA [26]. 15
- Fig. 1.9 Common relationship of temperature and time, for 200 mm anode, with various clinical operations [44]. 16
- Fig. 1.10 Speculated fracture process of anode target of x-ray tube. 18

Fig. 1.11 Typical relationship between temperature and time in the focal track of a rotating anode x-ray target during a clinical exposure.	19
Fig. 1.12 Fracture toughness of pure tungsten W (Δ), W-5%Re (\bullet), and W-10%Re (O) alloys [42].	20
Fig. 1.13 Relationship of fracture toughness and testing temperatures, at a temperature range of -150 °C and 450 °C [59].	21
Fig. 1.14 The S-N curves of Mo ₂ SiB alloy at 20 °C and 1200 °C. As a comparison, S-N curve of TZM at room temperature is shown [62].	24
Fig. 1.15 The comparison of the fatigue behavior of 713LC alloy and TZM alloy at 850 °C [71].	24
Fig. 1.16 Tungsten low-cycle fatigue data at (a) 815 °C and (b) room temperature [73].	25
Fig. 1.17 The S-N curves for rolled and forged tungsten at 280 °C and 480 °C [37].	26

Chapter 2

Fig. 2.1 Optical micrographs of the TZM alloys, before, and after test at 800 °C and 1200 °C.	42
Fig. 2.2 EPMA analysis of the materials used (a) TZM-A36 (b) TZM-B36.	42
Fig. 2.3 SENB specimen used: (a) overview and (b) detail of notch (in mm).	43
Fig. 2.4 Relationship between J and Δa for TZM-B36 at 800 °C.	47

Fig. 2.5 Relationship between J_C and side-groove depth ratio for TZM-B36 at 800 °C. 47

Fig. 2.6 J_{IC} values for TZM-A25, TZM-A36, TZM-B25 and TZM-B36 at high temperatures ranged from 800 °C to 1200 °C. 50

Fig. 2.7 The hardness of TZM alloys measured after the high temperature tests. 50

Fig. 2.8 Fracture surface observation of TZM-A36 and TZM-B36, after fracture toughness test at room temperature, 800 °C, 1000 °C and 1200 °C, respectively. 53

Fig. 2.9 A schematic representation on potential crack appears in the typical x-ray tube target. (a) Case 1: Crack at the W-Re layer, and (b) Case 2: Crack propagates reach TZM substrate layer. 55

Chapter 3

Fig. 3.1 (a) Schematic view of the x-ray tube's target, and (b) relationship between temperature and time in the focal track of a rotating anode x-ray target during a typical clinical exposure. 61

Fig. 3.2 Optical micrographs of the layered W-Re/TZM, the bulk W-Re and TZM before and after test. 67

Fig. 3.3 Bending fatigue specimens used: (a) for layered W-Re/TZM, (b) for bulk TZM and W-Re. 69

Fig. 3.4 Relationship between maximum tensile stress and rigidity of the layered specimen, where the maximum tensile stress and rigidity are normalized by those of the specimen with height ratio of 0.83.	70
Fig. 3.5 Schematic loading mode in the four-point bending fatigue test (in mm).	71
Fig. 3.6 Schematic diagram of fatigue test and experimental setup for compliance measurement.	73
Fig. 3.7 Load-displacement curves at various number of cycles at 1000 °C for layered W-Re/TZM.	75
Fig. 3.8 Relationship between compliance and number of cycles at 1000 °C for layered W-Re/TZM.	75
Fig. 3.9 S-N curves for the four-point bending fatigue tests at room temperature.	77
Fig. 3.10 Fracture surface observations of (a) layered W-Re/TZM, (b) bulk W-Re and (c) bulk TZM tested at room temperatures (upper: low magnification, lower: high magnification).	78
Fig. 3.11 S-N curve for the four-point bending fatigue tests at 1000 °C, where the fatigue failure is defined when the specimen compliance increases up to two-times of initial one.	80
Fig. 3.12 Examples of intergranular surface cracks observed on the specimen surfaces of (a) layered W-Re/TZM, (b) bulk W-Re, (c) bulk TZM, and (d) shows multiple crack nucleation on the specimen surface of bulk W-Re.	81

Fig. 3.13 Surface crack nucleation and propagation behavior during fatigue tests of the layered W-Re/TZM at 1000 °C; (a) maximum crack length, (b) number of cracks per area, and (c) total crack length per area. 83

Fig. 3.14 Fatigue crack depth after the test at 1000 °C and 10^6 fatigue cycles. (a) W-Re layer of layered W-Re/TZM, (b) bulk W-Re, and (c) bulk TZM. 86

Fig. 3.15 SEM observations of interfacial area between W-Re and TZM for layered W-Re/TZM specimens (a) before test, and (b) after fatigue test at 1000 °C (292 MPa, 10^6 cycles). Note: In the figure, upper part is W-Re, while below part is TZM. 87

Fig. 3.16 Vickers hardness of the three materials after the test at 1000 °C. 88

Fig. 3.17 Relationship between number of cycles spent in the test at 1000 °C and remaining fatigue life at room temperature. Marks put to symbols are indicated in Table 3.6. 93

Fig. 3.18 Fracture surface observation of (a) bulk W-Re, (b) layered W-Re/TZM and (c) bulk TZM specimens tested at room temperatures, after fatigue test at 1000 °C (upper: low magnification, lower: high magnification). 94

List of Tables

Chapter 1

Table 1.1 Comparison of some physical properties for pure refractory metals [4].	2
Table 1.2 Property comparison of Molybdenum and TZM alloy [5].	4
Table 1.3 Fracture toughness results for W-26%Re alloy, tested at different temperatures for recrystallized and as-forged condition [13].	22

Chapter 2

Table 2.1 Chemical composition for the TZM alloys used (mass %).	41
Table 2.2 Room temperature mechanical properties of the TZM alloys.	41

Chapter 3

Table 3.1 List of reported fatigue strengths for Mo alloys and W alloys.	64
Table 3.2 Chemical composition for the W-Re and TZM alloys used (mass%).	66
Table 3.3 Room temperature Vickers hardness for the materials used.	67
Table 3.4 Comparison of average grain size and average indentation size during Vickers hardness test for the materials used.	67
Table 3.5 The evaluated compliances for the specimens before fatigue tests.	74
Table 3.6 Remaining fatigue life at room temperature after fatigue test at 1000 °C.	90

List of Publications and Conferences

Publications:

1. Mohd Azhar HARIMON, Nafisah Arena HIDAYATI, Yukio MIYASHITA, Yuichi OTSUKA, Yoshiharu MUTOH and Shinichi YAMAMOTO, “*High temperature fracture toughness of TZM alloys with different kinds of grain boundary particles*”, International Journal of Refractory Metals and Hard Materials 66 (2017) 52-56.
2. Mohd Azhar HARIMON, Yukio MIYASHITA, Yuichi OTSUKA, Yoshiharu MUTOH and Shinichi YAMAMOTO, “*High temperature fatigue characteristics of P/M and hot-forge W-Re and TZM for x-ray target of CT scanner*”, Materials and Design 137 (2018) 335-344.

International Conference:

1. Mohd Azhar HARIMON, Nafisah Arina HIDAYATI, Yukio MIYASHITA, Yuichi OTSUKA, Yoshiharu MUTOH and Shinichi YAMAMOTO, “*Effect of Forging Ratio on High Temperature Fracture Toughness in TZM Alloy*”, International Conference on Advanced Technology in Experimental Mechanics 2015 (ATEM'15), Toyohashi, Japan (October 4-8, 2015).
2. Mohd Azhar HARIMON, Nafisah Arina HIDAYATI, Yukio MIYASHITA, Yuichi OTSUKA, Yoshiharu MUTOH, Hitoshi AOYAMA and Shinichi YAMAMOTO, “*High temperature fracture toughness estimation of TZM alloys using the convenient J_{IC} test method*”. Poster presented at International Symposium on Local Innovative Activation by Food and Energy (ISLife2017), Kagoshima, Japan (March 17-19, 2017).

National Conference:

1. Mohd Azhar HARIMON, Yukio MIYASHITA, Yuichi OTSUKA, Yoshiharu MUTOH, Hitoshi AOYAMA and Shinichi YAMAMOTO, “*Effect of Distribution in Precipitation on High Temperature Fracture Toughness of TZM Alloy*”, Japan Society of Mechanical Engineers Hokuriku Shin-Etsu Branch 53 General Assembly and Lectures, Nagano, Japan (March 5, 2016).

Chapter 1

Introduction

1.1 Introduction to refractory metals

For some decades, machines and equipment for high temperature operation have been developed with increasing demand for operating at a higher temperature, such as in industries, engineering and constructions, aerospace, power generations, etc. All of these machines in common are using refractory materials, which can keep their strength at high temperature. A material during their service time on high temperature, will suffering a severe condition due to extreme thermal shock, mechanical load, and oxidation attacks [1]. Hence, to deal with this condition, materials must be chemically and physically strong at high temperatures. However, after a long period of usage all of those effects will lead to make some damage of material and fractured.

Refractory metals can be classified as metals that are outstandingly resistant to heat and wear. The most common definition includes metallic elements of niobium (Nb), molybdenum (Mo), tantalum (Ta), and tungsten (W) based on the criteria of body centered cubic (bcc) crystal structure and minimum melting temperature of 2200 K [2]. The latest finding its entry in this special category of metals is rhenium (Re) because of its high melting point close to tungsten. All of these materials have some similarities in properties, such as a melting point higher than 2000 °C, high hardness at ambient temperature, chemically inert and have a relatively high density compared to other metals [3]. Table 1.1 shows a property comparison of Nb, Ta, Mo, W and Re.

Table 1.1 Comparison of some physical properties for pure refractory metals [4].

Property	Niobium	Tantalum	Molybdenum	Tungsten	Rhenium
Crystal structure	bcc	bcc	bcc	bcc	hcp
Density, g/cc	8.6	16.6	10.2	19.3	21.0
Melting point, °C	2470	3000	2620	3410	3170
Thermal expansion, (ppm/K)	7.3	6.3	4.8	4.5	6.2
Thermal conductivity (W/m. °K)	52	54	146	166	71
Modulus of elasticity at 20 °C (kN/mm ²)	100	190	320	400	460
Tensile strength (recrystallized) at 20 °C (N/mm ²)	200	300	500	700	800

1.1.1 Molybdenum

Molybdenum is one of the refractory metals which has been utilized as elevated temperature structural material as a result of its high melting temperature (2620 °C), high strength and creep resistance at high temperature. These excellent properties were provided by its body-centered cubic (bcc) structure which is stable at high temperature and high pressure [5]. Even though it has less oxidation resistant compared to tungsten, yet molybdenum possesses limited coefficient of thermal expansion, excellent heat resistance, as well as thermal conductivity. The moderate density also has made molybdenum appropriate employed as base for heat-resistant materials [6].

1.1.1.1 TZM alloy

When higher temperature strength is needed, titanium-zirconium-molybdenum (TZM) alloy has shown potential as the candidate material. TZM is widely used as material for high temperature application with heavy mechanical load, dies and cores for the die casting, extrusion as well as forging dies, and other high temperature applications when high temperature strength is required such as a base material of x-ray tube's anode target [1,6,7]. TZM alloy consists of (0.40–0.55) wt.% Ti, (0.06–0.12) wt.% Zr, (0.01–0.04) wt.% very fine carbides C and Mo in balance. Alloying molybdenum with Ti and Zr has shown significant increasing of high temperature strength (720 MPa), higher recrystallization temperature (1100 °C) and better creep resistance compared with pure molybdenum. The small amount addition of Ti and Zr has strengthened Mo solid solution due to the dispersion of composite carbides in the molybdenum matrix by the formation

of precipitates of TiC and ZrC [1,6]. Table 1.2 shows the basic mechanical properties of molybdenum in comparison with TZM alloy.

Table 1.2 Property comparison of Molybdenum and TZM alloy [5].

Nominal alloy addition, wt.%	Common designation	Usual condition	Low temp. ductility	Typical high-temperature strength			
				Temp., °C	Tensile, MPa	Temp., °C	10 h rupture, MPa
None	Unalloyed Mo ^(c)	S-R-A	B-C	1000	50	980	175
0.5Ti, 0.08 Zr, 0.03 C	TZM ^(c)	S-R-A	B-C	1000	600	1315	140

*S-R-A : stress relieved annealed, B : excellent RT ductility, C : may have marginally ductility at RT, ^(c) : available in both powder metallurgy and arc cast forms.

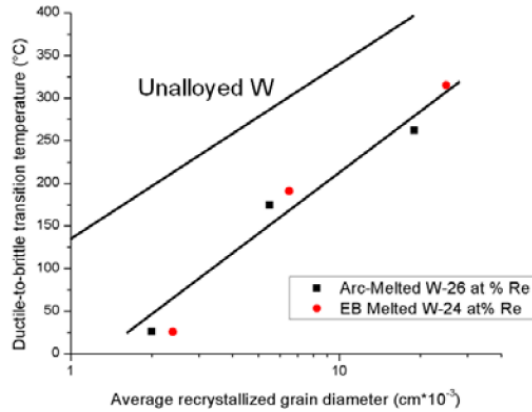
1.1.2 Tungsten

Tungsten (W) is the material with the highest melting temperature of all metals ($T_{\text{melting}} = 3410\text{ }^{\circ}\text{C}$) [8] and for that reason has been used as many decades in elevated temperature utilizations [9]. Tungsten alloys have become the best candidate for very high temperature functions due to their thermal capabilities as well as excellent elevated temperature mechanical properties. These properties also consist of low vapour pressure, high emissivity, and exceptional high-temperature rigidity and strength. In contrary, the exceptional elevated temperature properties of tungsten are compensate by obstacles in preparation as well as manufacturing due to its high melting temperature and low ductility at room temperatures [10].

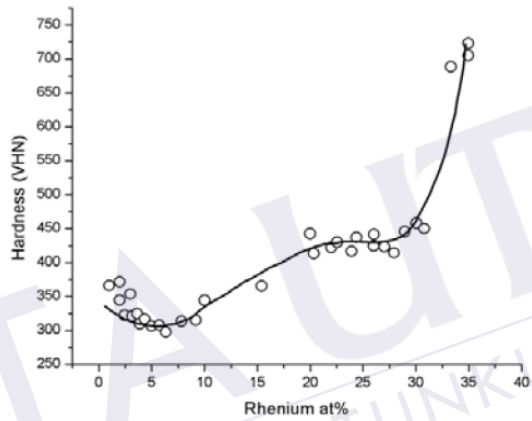
1.1.2.1 Tungsten-rhenium alloy

Research works have been conducted to produce tungsten alloys with enhanced low temperature manufacturing ability and elevated temperature mechanical properties as nuclear and aerospace utilizations, in an effort to overcome some of the problems. It has been established that a limited addition of rhenium able to enhance the tungsten's ductility at low temperature and strength at elevated temperature [10]. The rhenium addition to tungsten revealed a significant reduction in the ductile to brittle transition temperature (DBTT), and finer grained materials furthermore cause to the needed reduce in the DBTT as presented in Fig. 1.1(a) [11].

In addition, purity, surface condition, strain rate and also testing environment (for example, high temperature) likely to affect DBTT. Hardness results of pure tungsten and W-Re alloys with different compositions are presented in Fig. 1.1 (b). It can be observed that there exists a particular reaction, where at lesser Re concentrations (5 to 15 at.%), solid softening effect occurs before it starts strengthening the matrix metal at higher concentrations. The better ductility is accomplished by so called 'rhenium ductilizing effect' where Re generates substantial twinning and a raise in the number of slip planes [11]. In the succeeding decades, the research works on fatigue and fracture behavior of tungsten-rhenium alloys is quite rare, which possibly associated to the reality that rhenium is a very hard to find and thereby high-priced metal. It is not targeted to be utilized at high concentrations at a broad or in industry scale. Nonetheless, because of its high density and high atomic number (Z), it is widely used in medical x-ray devices as an anode target [12,13].



(a)



(b)

Fig. 1.1. (a) Relationship of DBTT and average recrystallized grain diameter for pure tungsten and W-24Re/W-26Re and (b) relationship of Vickers hardness (VHN) and rhenium content [11].

1.1.3 Fabricating process of refractory metals

Given all the interesting features of refractory metals, it is important to establish appropriate fabrication procedures for tungsten and molybdenum alloys. Given the high melting points of the constituents, it was unrealistic to consider the conventional solidification process of casting as the fabrication route. Work in the 1960s and 1970s

used materials that produce by vacuum arc remelting (VAR) as well as electron beam melting (EBM) techniques which purity were suspected [11].

Tungsten and molybdenum alloys are commonly fabricated by powder metallurgy methods as casting ingots is a difficult and expensive process due to its high melting temperature [14,15]. The isothermal powder metallurgy process begins with consolidation of the powder by pressing at room temperature become rods and plates with different geometries and sizes. Conventionally, sintering is conducted by giving outside pressure such as Hot-Isostatic-Pressing (HIP). The process of sintering is conducted in furnaces at elevated temperatures (normally in the temperature range of 1800 to 2200 °C) and in hydrogen environment in some duration of time (2 to 3 hours) to earn densities around 90% of theoretical density [16]. Hot rolling, extrusion or forging at temperatures between 1200 to 1500 °C are afterward used for higher densities. Spark plasma sintering (SPS) is a recent technology for compression of metal powders. It has a brief time for sintering process, where metal powders are compacted by pressing and heating at the same time from a pulsed electric field. Compared to conventional sintering methods, densification by SPS is very quick. Hence, the sintering temperatures can be reduced which it can inhibit the grain growth [16].

Recently, metal injection molding (MIM) also has been used to produce tungsten and molybdenum alloys [17]. Additive manufacturing type of powder metallurgy also can be applied, such as selective laser sintering (SLS) [18], selective laser melting (SLM) [19] as well as electron beam melting (EBM) [20]. Figure 1.2 shows the typical fabrication processes of Mo and W products.

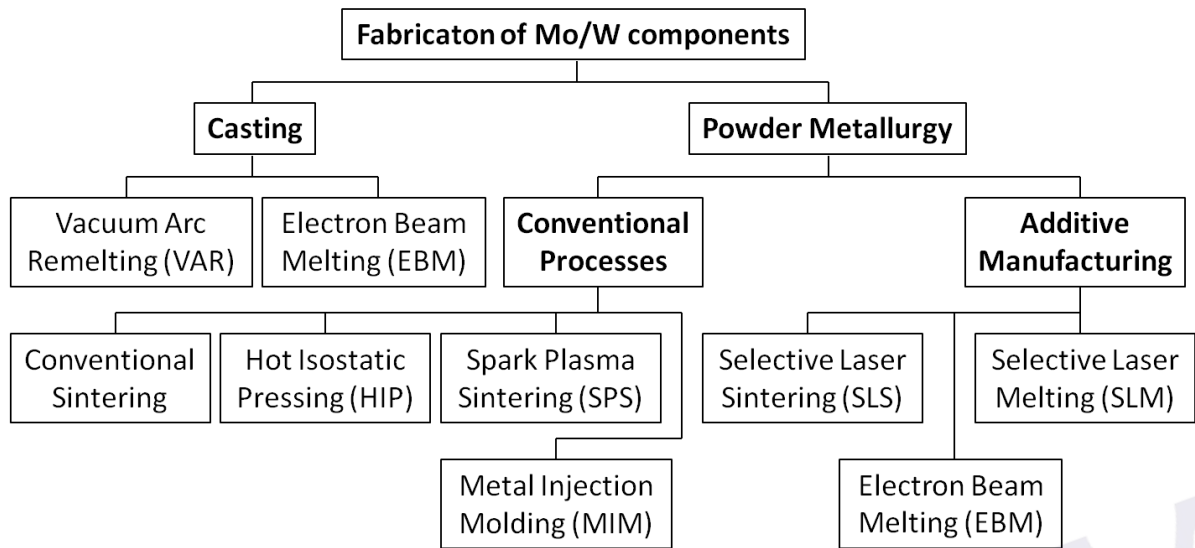


Fig. 1.2 Fabrication processes of Mo and W components.

1.2 Application of refractory metals

Refractory metals and their alloys are able of satisfying an aggressive environment with respect to radiation, temperature, corrosion and stress for extended periods. These materials are thus being studied as high temperature structural materials, for current generation reactors like accelerator driven system (ADS), compact high temperature reactor (CHTR), advanced heavy water reactor (AHWR), fusion equipments [21,22] and space aircrafts [23]. There is an expanding interest for materials that able to sustain reliability under developing temperature environments. Above 1200K, the refractory metal alloys are particularly possible choice elements as structural use. Fig. 1.3 demonstrates the possible choice materials with increasing operational temperatures, in the application of nuclear power systems [3].

References

- [1] H. Walser, J.A. Shields, Traditional and emerging applications of molybdenum metal and its alloys, July, IMOA Newsletter, International Molybdenum Association, London, 2007.
- [2] J.A. Shields, Applications of Molybdenum Metal and its Alloys, Second, International Molybdenum Association, London, 2013.
- [3] M.R. Eggleston, M.R. Jackson, M.G. Benz, G. Reznikov, Joining ductile refractory metal inserts in x-ray tube targets, JOM. 48 (1996) 59–64.
- [4] A.A. Khan, J.C. Labbe, A. Grimaud, P. Fauchais, Molybdenum and tungsten coatings for x-ray targets obtained through the low-pressure plasma spraying process, J. Therm. Spray Technol. 6 (1997) 228–234.
- [5] A.A. Khan, J.C. Labbe, Advanced ceramic matrix composites for high energy x-ray generation, Adv. Nat. Sci. Nanosci. Nanotechnol. 2 (2012) 45015.
- [6] A.S. Gontar, M.L. Taubin, E.E. Konoplev, Estimation of service life of x-ray tube anodes, Biomed. Eng. (NY). 46 (2013) 190–193.
- [7] J. Habainy, S. Iyengar, Y. Lee, Y. Dai, Fatigue behavior of rolled and forged tungsten at 25°, 280° and 480 °C, J. Nucl. Mater. 465 (2015) 438–447.
- [8] F. Jiang, Y. Zhang, N. Sun, J. Leng, Tungsten coating prepared on molybdenum substrate by electrodeposition from molten salt in air atmosphere, Appl. Surf. Sci. 327 (2015) 432–436.

- [9] M.A. Harimon, N.A. Hidayati, Y. Miyashita, Y. Otsuka, Y. Mutoh, S. Yamamoto, H. Aoyama, High temperature fracture toughness of TZM alloys with different kinds of grain boundary particles, *Int. J. Refract. Met. Hard Mater.* 66 (2017) 52–56.
- [10] Y. Mutoh, K. Ichikawa, K. Nagata, M. Takeuchi, Effect of rhenium addition on fracture-toughness of tungsten at elevated temperatures, *J. Mater. Sci.* 30 (1995) 770–775.
- [11] S. Wurster, B. Gludovatz, R. Pippan, High temperature fracture experiments on tungsten–rhenium alloys, *Int. J. Refract. Met. Hard Mater.* 28 (2010) 692–697.
- [12] P.L. Raffo, Yielding and fracture in tungsten and tungsten-rhenium alloys, *J. Less Common Met.* 17 (1969) 133–149.
- [13] T. Leonhardt, Properties of tungsten-rhenium and tungsten-rhenium with hafnium carbide, *JOM J. Miner. Met. Mater. Soc.* 61 (2009) 68–71.
- [14] J.L. Taylor, Tensile properties of tungsten-3% rhenium from 1400° to 2900°C in vacuum, *J. Less Common Met.* 7 (1964) 278–287.
- [15] W.D. Klopp, P.L. Raffo, W.R. Witzke, Mechanical properties of dilute tungsten-rhenium alloys, NASA Technical Note NASA TN D-3483, Washington, DC, 1966.
- [16] K.S. Shin, A. Luo, B.-L. Chen, D.L. Jacobson, High-temperature properties of particle-strengthened W-Re, *JOM.* 42 (1990) 12–15.
- [17] J. Warren, The 700° C tensile behavior of Mo-0.5 Ti-0.08 Zr-0.025 C (TZM) extruded bar measured transverse and parallel to the billet extrusion axis, *Int. J.*

- Refract. Met. Hard Mater. 16 (1998) 149–157.
- [18] M. Nagae, T. Yoshio, J. Takada, Y. Hiraoka, Improvement in recrystallization temperature and mechanical properties of a commercial TZM alloy through microstructure control by multi-step internal nitriding, Mater. Trans. 46 (2005) 2129–2134.
- [19] B.V. Cockeram, The mechanical properties and fracture mechanisms of wrought low carbon arc cast (LCAC), molybdenum–0.5pct titanium–0.1pct zirconium (TZM), and oxide dispersion strengthened (ODS) molybdenum flat products, Mater. Sci. Eng. A. 418 (2006) 120–136.
- [20] T. Mroczek, A. Hoffmann, U. Martin, Hardening mechanisms and recrystallization behaviour of several molybdenum alloys, Int. J. Refract. Met. Hard Mater. 24 (2006) 298–305.
- [21] K.-S. Wang, J.-F. Tan, P. Hu, Z.-T. Yu, F. Yang, B.-L. Hu, R. Song, H.-C. He, A.A. Volinsky, La₂O₃ effects on TZM alloy recovery, recrystallization and mechanical properties, Mater. Sci. Eng. A. 636 (2015) 415–420.
- [22] A.P. Alur, K.S. Kumar, Monotonic and cyclic crack growth response of a Mo–Si–B alloy, Acta Mater. 54 (2006) 385–400.
- [23] A. Ferro, P. Mazzetti, G. Montalenti, On the effect of the crystalline structure on fatigue- Comparison between body-centred metals (Crystalline structure on fatigue noting changes of body-centred metals and face-centred and hexagonal metals), Philos. Mag. 8 TH Ser. 12 (1965) 867–875.

- [24] P. Beardmore, P.H. Thornton, Fatigue fracture in polycrystalline molybdenum, *Acta Metall.* 18 (1970) 109–115.
- [25] P. Beardmore, P.H. Thornton, The relationship between discontinuous yielding and cyclic behavior in polycrystalline molybdenum, *Metall. Trans.* 1 (1970) 775–779.
- [26] J.A. Roberson, Environmental influences of the fatigue of molybdenum, *Trans. Metall. Soc. AIME.* 233 (1965) 1799.
- [27] W. Hoffelner, C. Wuethrich, G.H. Gessinger, G. Schroeder, TZM molybdenum as a die material for isothermal forging of titanium alloys, *High Temp High Press.* 14 (1982) 33–40.
- [28] H.A. Calderon, G. Kostorz, G. Ullrich, Microstructure and plasticity of two molybdenum-base alloys (TZM), *Mater. Sci. Eng. A.* 160 (1993) 189–199.
- [29] C.R. Honeycutt, T.F. Martin, J.C. Sawyer, E.A. Steigerwald, Elevated temperature fatigue of TZC molybdenum alloy under high frequency and high vacuum conditions. Topical Report No. 1., 1967.
- [30] H.-J. Shi, C. Korn, G. Pluinage, High temperature isothermal and thermomechanical fatigue on a molybdenum-based alloy, *Mater. Sci. Eng. A.* 247 (1998) 180–186.
- [31] W. Jakobeit, J.-P. Pfeifer, G. Ullrich, Evaluation of high-temperature alloys for helium gas turbines, *Nucl. Technol.* 66 (1984) 195–206.
- [32] W. Jakobeit, PM Mo-TZM Turbine Blades--Demands on Mechanical Properties, *Int. J. Refract. Hard Met.* 2 (1983) 133–136.

- [33] R.E. Schmunk, G.E. Korth, Tensile and low-cycle fatigue measurements on cross-rolled tungsten, *J. Nucl. Mater.* 103&104 (1981) 943–947.
- [34] P. Lorenzo, M. Miralda, S. Iyengar, S. Melin, E. Noah, Fatigue properties and characterization of tungsten heavy alloys IT180 & D176, *Int. J. Refract. Met. Hard Mater.* 41 (2013) 250–258.
- [35] A.J. Sunwoo, D.C. Freeman, W. Stein, V.K. Bharadwaj, D.C. Shultz, J.C. Sheppard, Characterization of W-26%Re Target Material, Linear Collider Collaboration Tech Notes, LCC-0103, UCRL-JC- 149787, 2002.
- [36] H. Aoyama, S. Yamamoto, Y. Miyashita, Y. Mutoh, Microstructure, high temperature strength and CO-gas emission of liquid-phase sintered and forged low oxygen TiC-ZrC-Mo alloy, *Journal-Society Mater. Sci. Japan.* 55 (2006) 558–562.
- [37] ASTM B387, Standard Specification for Molybdenum and Molybdenum Alloy Bar, Rod, and Wire, ASTM International, 2001.
- [38] R.C. Hibbeler, Bending, in: *Mech. Mater.*, Seventh Ed, Prentice Hall, New Jersey, 2008: pp. 254–361.
- [39] B. V Cockeram, Measuring the Fracture Toughness of Molybdenum-0.5 pct Titanium-0.1 pct Zirconium and Oxide Dispersion – Strengthened Molybdenum Alloys using Standard and Subsize Bend Specimens, *Metall. Mater. Trans. A.* 33 (2002) 3685–3707.
- [40] ASTM E606 / E606M-12, Standard Test Method for Strain-Controlled Fatigue Testing, ASTM International, 2012.

- [41] Japan Industrial Standard JIS Z 2279 : Method of high temperature low cycle fatigue testing for metallic materials, Japanese Standards Association, 1992.
- [42] V. Shankar, V. Bauer, R. Sandhya, M.D. Mathew, H.-J. Christ, Low cycle fatigue and thermo-mechanical fatigue behavior of modified 9Cr--1Mo ferritic steel at elevated temperatures, *J. Nucl. Mater.* 420 (2012) 23–30.
- [43] A. Nagesha, M. Valsan, R. Kannan, K.B.S. Rao, S.L. Mannan, Influence of temperature on the low cycle fatigue behaviour of a modified 9Cr--1Mo ferritic steel, *Int. J. Fatigue*. 24 (2002) 1285–1293.
- [44] C. Kanchanomai, S. Yamamoto, Y. Miyashita, Y. Mutoh, A.J. McEvily, Low cycle fatigue test for solders using non-contact digital image measurement system, *Int. J. Fatigue*. 24 (2002) 57–67.
- [45] H. Solomon, Fatigue of 60/40 solder, *IEEE Trans. Components, Hybrids, Manuf. Technol.* 9 (1986) 423–432.
- [46] J.H.L. Pang, B.S. Xiong, T.H. Low, Low cycle fatigue study of lead free 99.3 Sn--0.7 Cu solder alloy, *Int. J. Fatigue*. 26 (2004) 865–872.
- [47] S. Tarafder, M. Tarafder, V.R. Ranganath, Compliance crack length relations for the four-point bend specimen, *Eng. Fract. Mech.* 47 (1994) 901–907.
- [48] P.M. Cheng, Z.J. Zhang, G.J. Zhang, J.Y. Zhang, K. Wu, G. Liu, W. Fu, J. Sun, Low cycle fatigue behaviors of pure Mo and Mo-La₂O₃ alloys, *Mater. Sci. Eng. A*. 707 (2017) 295–305.
- [49] H. Kurishita, Y. Kitsunai, T. Shibayama, H. Kayano, Y. Hiraoka, Development of

Mo alloys with improved resistance to embrittlement by recrystallization and irradiation, J. Nucl. Mater. 233 (1996) 557–564.

- [50] D. Wolfarth, P. Ducheyne, Effect of a change in interfacial geometry on the fatigue strength of porous-coated Ti-6Al-4V, J. Biomed. Mater. Res. Part A. 28 (1994) 417–425.

